Analytic expressions for ANU BEC collision experiment

R. J. Lewis-Swan[1,2]

[1] *Homer L. Dodge Department of Physics and Astronomy, The University of Oklahoma, Norman, Oklahoma 73019, USA*

[2] *Center for Quantum Research and Technology, The University of Oklahoma, Norman, Oklahoma 73019, USA*

(Dated: August 2, 2021)

We compute integrated correlation functions for a Rarity-Tapster scheme based on correlated atom pairs generated by four-wave mixing in colliding BECs. We focus on the collision configuration of the current ANU experiment and highlight differences to the previously considered setup of Phys. Rev. A 91, 052114 (2015). We comment on the potential implications for the experimental observation of a violation of a CHSH-Bell inequality.

I. SETUP OF THE PROBLEM

We seek to compute the integrated pair-correlation function,

$$C_{ij} = \int_{V(\mathbf{k}_i)} d^3\mathbf{k} \int_{V(\mathbf{k}_j)} d^3\mathbf{k}'\ G^{(2)}(\mathbf{k},\mathbf{k}'), \tag{1}$$

at the output of a Rarity-Tapster protocol. This integrated quantity intrinsically depends on the nature of the two-point correlation function, which in Ref. [1] is assumed to be of the form,

$$\frac{G^{(2)}(\mathbf{k},\mathbf{k}')}{\bar{n}^2} = 1+\frac{h}{2}\left[1 \pm \cos(\Phi+\varphi(\mathbf{k},\mathbf{k}'))\right]\prod_d e^{-(\mathbf{k}+\mathbf{k}')^2/2\sigma_d^2}. \tag{2}$$

Here, σ_d is the original back-to-back (BB) correlation length and h the correlation strength. The correlation is normalized by the nominally constant halo population density $\bar{n}$. The phase-shifts of the Rarity-Tapster scheme are encoded in Φ (e.g., $\Phi = \phi_L \pm \phi_R$ depending on the details of the implementation) and $\varphi(\mathbf{k},\mathbf{k}')$ describes some phase-diffusion that occurs between scattered pairs with momenta $\mathbf{k} \neq -\mathbf{k}'$ [1].

The goal of these notes is to determine the equivalent version of Eq. (2) for the specific configuration of the ANU experiment, in particular the form of $\varphi(\mathbf{k},\mathbf{k}')$ and how it depends on the key parameters of experiment (e.g., BEC size, momentum kick, etc).

In Fig. 1 we present a comparison of the geometry of the current experiment relative to the original scheme proposed in Ref. [1]. We identify the momentum modes $\mathbf{k}_j$ for $j = 1, ..., 4$ that are involved in the Rarity-Tapster interferometer, and point out that the configuration of these modes slightly differs between the two possible protocols. In particular, modes $\mathbf{k}_2$ and $\mathbf{k}_4$ are switched [although correlations are preserved between the pairs $(\mathbf{k}_1,\mathbf{k}_2)$ and $(\mathbf{k}_3,\mathbf{k}_4)$]. Moreover, the targetted pairs are stationary along the $\hat{z}$-direction in the COM frame of each colliding pair. The former change leads to only superficial differences in our results, but the latter fundamentally alters the behaviour of the phase-sensitive correlation C_{ij}.

II. CALCULATING THE INTEGRATED CORRELATION FUNCTION

Without loss of generality, we will focus on a representative calculation of C_{12} for the ANU geometry, which means we must first derive $G^{(2)}(\mathbf{k},\mathbf{k}')$ for $\mathbf{k} \approx \mathbf{k}_1$ and $\mathbf{k}' \approx \mathbf{k}_2$ (see Fig. 1). Treating the Bragg pulses as instantaneous (and perfect) linear transformations, it is straightforward to adapt/rederive the result (B2) of Ref. [1]:

$$\begin{aligned} G^{(2)}(\mathbf{k},\mathbf{k}') = \bar{n}^2 + \frac{1}{4}\Big\{ & |m(\mathbf{k},\mathbf{k}',t_c) + |m(\mathbf{k}-2\mathbf{k}_L,\mathbf{k}'-2\mathbf{k}_L,t_c)|^2 \\ & - m(\mathbf{k}-2\mathbf{k}_L,\mathbf{k}'-2\mathbf{k}_L,t_c)^* m(\mathbf{k},\mathbf{k}',t_c) e^{-i\Phi + i\frac{2\hbar k_L}{m}[(\mathbf{k}+\mathbf{k}')_z - 2k_L]\Delta t_{\text{free}}} \\ & - m(\mathbf{k},\mathbf{k}',t_c)^* m(\mathbf{k}-2\mathbf{k}_L,\mathbf{k}'-2\mathbf{k}_L,t_c) e^{i\Phi - i\frac{2\hbar k_L}{m}[(\mathbf{k}+\mathbf{k}')_z - 2k_L]\Delta t_{\text{free}}}\Big\}, \end{aligned} \tag{3}$$

where $m(\mathbf{k},\mathbf{k}',t) = \langle \hat{a}(\mathbf{k},t)\hat{a}(\mathbf{k}',t)\rangle$ is the anomalous pair correlation, $2\mathbf{k}_L = k_0\hat{z}$ is the momentum imparted by the Bragg pulse, $k_L = |k_L|$, Δt_{free} is the free propagation time and t_c the initial collision duration.

In Appendix A we show that the anomalous moment can be well approximated by the form,

$$\begin{aligned} m(\mathbf{k},\mathbf{k}',t) = \bar{n}\sqrt{h}\Big[& e^{i\theta_+(\mathbf{k},\mathbf{k}',t)} \prod_d e^{-(k_d+k'_d-k_0\hat{z})^2/4\sigma_d^2} \\ & + e^{i\theta_-(\mathbf{k},\mathbf{k}',t)} \prod_d e^{-(k_d+k'_d+k_0\hat{z})^2/4\sigma_d^2}\Big]. \end{aligned} \tag{4}$$

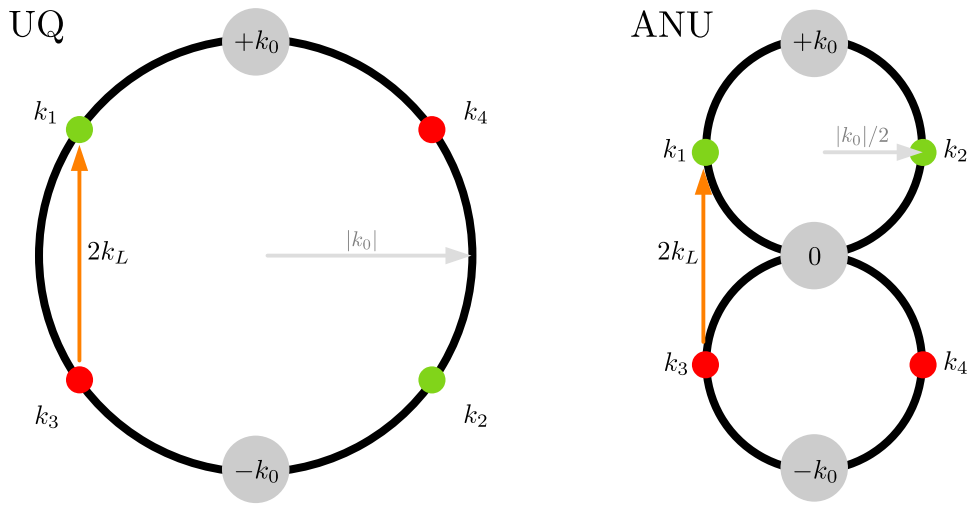

FIG. 1. Collision and Rarity-Tapster setup. (Left) The original UQ proposal involves only a single scattering halo (radius $|k_0|$ centered at $\mathbf{k}=0$) generated by the collision of a pair of BECs with COM momenta $\pm k_0\hat{z}$ (indicated by grey blobs). After the collision, strong atom-atom correlations are between pairs $(\mathbf{k}_1,\mathbf{k}_2)$ and $(\mathbf{k}_3,\mathbf{k}_4)$. The Rarity-Tapster scheme mixes instead the (uncorrelated) pairs $(\mathbf{k}_1,\mathbf{k}_3)$ and $(\mathbf{k}_2,\mathbf{k}_4)$. (Right) The ANU scheme involves two scattering halos (equal radius $|k_0|/2$ centered at $\mathbf{k}=\pm k_0\hat{z}$) generated by three colliding BECs with COM momenta $0,\pm k_0\hat{z}$. Again, we assume the correlated pairs after the collision are $(\mathbf{k}_1,\mathbf{k}_2)$ and $(\mathbf{k}_3,\mathbf{k}_4)$. However, notice that the relative location of the modes $\mathbf{k}_2$ and $\mathbf{k}_4$ have been interchanged relative to the UQ scheme.

Note that the correlation splits into two contributions corresponding to pairs in the upper and lower halos. The fixed amplitude, $|m(\mathbf{k},\mathbf{k}',t)|\propto\bar{n}\sqrt{h}$, is an approximation that is motivated by the fact we only consider detection volumes [see Eq. (1)] much smaller than the typical width of the scattering halo in momentum space.

The phase of the anomalous moment is given by,

$$\theta_{\pm}(\mathbf{k},\mathbf{k}',t)\simeq-\frac{\pi}{2}-\frac{\hbar}{2m}(k^2+k'^2)t + \frac{\sigma_{g,z}}{\sqrt{\pi}k_0}\left\{(k^2+k'^2)\mp k_0(k_z+k'_z)\right\}, \quad (5)$$

where $\sigma_{g,z}$ is the rms width of the density profile of the source BEC under the assumption it may be modelled as a Gaussian (see Appendix A for a more detailed discussion). The phase (modulo $\pi/2$) can be loosely understood as having two contributions. The first term describes the usual phase accrued due to the free particle dispersion $\propto k^2$. The second term, $\propto\sigma_{g,z}$, is similar to that previously derived in Ref. [1], and approximately describes a phase accrued due to an energy mismatch between the initial and final scattered pairs.

Substitution of Eq. (4) into Eq. (3) yields the new result,

$$\frac{G^{(2)}(\mathbf{k},\mathbf{k}')}{\bar{n}^2}-1=\frac{h}{2}\left[1\pm\cos(\Phi+\varphi(\mathbf{k},\mathbf{k}'))\right] \times\prod_d e^{-(\mathbf{k}+\mathbf{k}'-k_0)^2/2\sigma_d^2}, \quad (6)$$

with

$$\begin{aligned}\varphi(\mathbf{k},\mathbf{k}')&\equiv\theta_-(\mathbf{k}-2\mathbf{k}_L,\mathbf{k}'-2\mathbf{k}_L,t_c)-\theta_+(\mathbf{k},\mathbf{k}',t_c)\\&\quad+\frac{2\hbar k_L}{m}[(\mathbf{k}+\mathbf{k}')_z-2k_L]\Delta t_{\rm free},\\&=-4k_L\left[(\mathbf{k}+\mathbf{k}')_z-2k_L\right]\frac{\hbar}{2m}(\Delta t_{\rm free}-t_c). \quad (7)\end{aligned}$$

where we have used that $2k_L=k_0$.

Finally, we are ready to compute the integrated correlation function C_{ij} from the definitions of Eqs. (1) and (6). We find,

$$C_{ij}=\bar{n}^2V+\frac{\bar{n}^2h}{2}\left[1\pm\cos(\Phi)\right]\alpha_x\alpha_y\beta_z\prod_d\left(2\sigma_d^2\right), \quad (8)$$

with

$$\alpha_d=e^{-2\lambda_d^2}-1+\sqrt{2\pi}\lambda_d\mathrm{erf}(\sqrt{2}\lambda_d), \quad (9)$$

and β_d can be expressed in the compact form,

$$\begin{aligned}\beta_d&=e^{-2\lambda_d^2}\cos(4\mathcal{A}_d\lambda_d)-1+2\sqrt{2}\mathcal{A}_dD_{\rm F}\left(\sqrt{2}\mathcal{A}_d\right)\\&\quad+\sqrt{\frac{\pi}{2}}e^{-2\mathcal{A}_d^2}\Big[(\lambda_d-i\mathcal{A}_d)\mathrm{erf}\left(\sqrt{2}\lambda_d-\sqrt{2}i\mathcal{A}_d\right)\\&\quad+(\lambda_d+i\mathcal{A}_d)\mathrm{erf}\left(\sqrt{2}\lambda_d+\sqrt{2}i\mathcal{A}_d\right)\Big], \quad (10)\end{aligned}$$

where we define $\mathcal{A}_d=(k_L\sigma_d\hbar/m)(\Delta t_{\rm free}-t_c)$.

III. COMPARISON TO PRIOR WORK AND THE ROLE OF INDISTINGUISHABILITY

It is important at this point to pause and discuss in more detail the differences between the results (**??**)-(**??**) we have obtained for the ANU configuration, as opposed to those of the original UQ configuration. In the following we demonstrate that in fact all quantitative differences between the two configurations can be elegantly traced back to the simple, intuitive requirement that the scattered pairs trace out paths through the Rarity-Tapster interferometer that are *indistinguishable*.

The central difference between the UQ and ANU configurations is the form of the phase term $\varphi(\mathbf{k},\mathbf{k}')$. We have usually understood this term as a type of dephasing between momentum modes that accrued different phase shifts during free propagation, and which scrambles the phase-settings of the Rarity-Tapster scheme and degrades any potential observation of a violation of the CHSH-Bell inequality.

For completeness, the result for $\varphi(\mathbf{k},\mathbf{k}')$ in the UQ configuration is,

$$\varphi(\mathbf{k},\mathbf{k}') = -4k_L\left[(\mathbf{k}-\mathbf{k}')_z - 2k_L\right] \times\left[\frac{\hbar}{2m}(\Delta t_{\rm free}-t_c)+\frac{m\sigma_{g,z}}{2k_0\sqrt{\pi}}\right] \quad (11)$$

Superficially, the result deviates from Eq. (7) as it depends on $(\mathbf{k}-\mathbf{k}')$. However, this does not lead to important quantitative differences. Instead, the key difference is the additional contribution $\propto m\sigma_{g,z}/(2k_0\sqrt{\pi})$, which motivated the definition of an optimal free propagation time $\Delta t_{\rm free} = t_c - m\sigma_{g,z}/(2k_0\sqrt{\pi})$ such that $\varphi(\mathbf{k},\mathbf{k}')=0$. To understand why this differentiating term appears in the UQ configuration and not the ANU configuration, it is illuminating to realize we can rewrite Eq. (11) in terms of the separation time, $t'_{\rm sep}=\sigma_{g,z}m/(\hbar k_0)$, as:

$$\varphi(\mathbf{k},\mathbf{k}') = -\frac{2\hbar k_L\left[(\mathbf{k}-\mathbf{k}')_z-2k_L\right]}{m} \times\left[(\Delta t_{\rm free}-t_c)+\frac{t'_{\rm sep}}{\sqrt{\pi}}\right]. \quad (12)$$

Thus, the shift in the optimal free propagation time is simply shifted (up to some prefactor) by the time it takes for the BECs to split.

But why is this separation time present in the UQ result but not that for the ANU configuration? In the following, we will demonstrate that Eq. (12) reflects the fact that we require the scattered pairs arrive at the final beam-splitter with maximum spatial overlap, which is essential to retain indistinguishability of the scattered pairs and thus observe phase-sensitive interference in the coincidence counts C_{ij}. Similarly, the *lack* of this term in the ANU result (7) is due to precisely the same condition!

To elucidate this point, we will use a simple toy model that treats the scattered pairs as classical particles that are randomly generated during the BEC collision. By tracing out the classical trajectories of each pair, we are able to *precisely* deduce the optimal free propagation time $\Delta t_{\rm free}$ that maximizes the spatial overlap of the particles at the final beam-splitter, and thus explain the form of $\varphi(\mathbf{k},\mathbf{k}')$ for each configuration.

A. Classical particle model: UQ configuration

We consider pair production due to the colliding BECs as a classical stochastic process. To construct our toy model it is first necessary to revisit some key points of the full quantum problem. In particular, we highlight that pair creation (scattering) term of the Hamiltonian within the Bogoliubov approximation is driven by the spatially and temporally modulated effective source $g(\mathbf{r},t)=2U_0\psi_+(\mathbf{r},t)\psi_-(\mathbf{r},t)$ where

$$\psi_\pm(\mathbf{r},t)=\sqrt{\frac{\rho_0}{2}}e^{\pm ik_0z-i\frac{\hbar k_0^2}{2m}t}e^{-\frac{x^2}{2\sigma_{g,x}^2}-\frac{y^2}{2\sigma_{g,y}^2}-\frac{(z\mp v_0t)^2}{2\sigma_{g,z}^2}}. \quad (13)$$

Two salient features of $g(\mathbf{r},t)$ are that: i) it is peaked at $\mathbf{r}=0$ (due to the symmetry of the BECs splitting in opposing directions at equal velocities), and ii) it decays in time with an envelope $g(\mathbf{r},t)\sim e^{-(t/t_{\rm sep})^2}$ where $t'_{\rm sep}=m\sigma_{g,z}/(\hbar k_0)$ is the typical timescale for the Gaussian source condensates to spatially separate.

As a result of these points, we adopt a crude classical description where pairs of point[1] particles are 'born' at the origin $\mathbf{r}=0$ at some time $0\leq t_{\rm birth}\lesssim t_{\rm sep}$. Each pair is composed of particles with opposing momenta $\pm\mathbf{k}$ such that energy and momentum conservation are preserved in the scattering process (i.e., those that lie on the usual scattering halo). For simplicity, we will focus our discussion on pairs with momenta $(\mathbf{k}_1,\mathbf{k}_2)$ and $(\mathbf{k}_3,\mathbf{k}_4)$ where $\mathbf{k}_1=-\mathbf{k}_2=(-k_0,k_0)/\sqrt{2}$ and $\mathbf{k}_3=-\mathbf{k}_4=(-k_0,-k_0)/\sqrt{2}$, which correspond to the targetted momentum modes of the archetypal atomic Rarity-Tapster scheme.

With the setup of the model accomplished, let us now turn our consideration to the problem of indistinguishability in the Rarity-Tapster interferometer. Intuitively, we expect that to observe strong interference fringes in the coincidence counts at the outputs of the final beam-splitter the paths traced out by the pairs being mixed must be indistinguishable. This can be equivalently phrased as requiring that our classical particles arrive at the final beam-splitter at an identical location and time (albeit independently as, in the limit of weak scattering, only one pair should exist in any one shot of the experiment). Clearly, when considering the notion of arriving at the same point in space we should keep in mind that in

[1] It is straightforward to imaging the particles are instead, e.g., Gaussian wavepackets of finite spatial width and the following analysis is simply for the position of their peak density.

the real quantum problem the particles are wavepackets with a finite spatial width, and thus all that we really need is for the particles to arrive sufficiently close together (i.e., within a coherence length).

This condition of indistinguishability sets some simple conditions on the relation between the initial collision duration t_c (the conclusion of which defines when the mirror Bragg pulse is applied) and the free propagation time $\Delta t_{\rm free}$ (after which the beam-splitter Bragg pulse is applied). To elucidate this, first consider a situation where the pairs are only created at $t = 0$. Computing the classical trajectories of the particles it is straightforward to obtain the spatial positions $\mathbf{r}_j$ where $j = 1, ..., 4$ identifies the initial particles with momenta $\mathbf{k}_1, ..., \mathbf{k}_4$:

$$\begin{aligned}
\mathbf{r}_1 &= \left(-\frac{v_0}{\sqrt{2}}[\Delta t_{\rm free} + t_c], -\frac{v_0}{\sqrt{2}}[\Delta t_{\rm free} - t_c]\right), \\
\mathbf{r}_2 &= \left(\frac{v_0}{\sqrt{2}}[\Delta t_{\rm free} + t_c], \frac{v_0}{\sqrt{2}}[\Delta t_{\rm free} - t_c]\right), \\
\mathbf{r}_3 &= \left(-\frac{v_0}{\sqrt{2}}[\Delta t_{\rm free} + t_c], \frac{v_0}{\sqrt{2}}[\Delta t_{\rm free} - t_c]\right), \\
\mathbf{r}_4 &= \left(\frac{v_0}{\sqrt{2}}[\Delta t_{\rm free} + t_c], -\frac{v_0}{\sqrt{2}}[\Delta t_{\rm free} - t_c]\right),
\end{aligned} \tag{14}$$

where $v_0 = \hbar k_0/m$. The trajectories traced out by each pair for this scenario are indicated by the faded lines in Fig. 2.

For indistinguishability we desire that, e.g., $d_{13} = |\mathbf{r}_1 - \mathbf{r}_3|$ and $d_{24} = |\mathbf{r}_2 - \mathbf{r}_4|$ are sufficiently small such that we cannot discriminate between the pairs. It is straightforward to compute,

$$d_{13}^2 = d_{24}^2 = v_0^2(\Delta t_{\rm free} - t_c)^2, \tag{15}$$

which vanishes for $\Delta t_{\rm free} = t_c$. This makes intuitive sense: The opposing pairs originate from the same location with opposite velocity along $\hat{y}$ and will be brought back together if the time between the origin and mirror is identical to that between the mirror and beam-splitter.

Now, let us instead think about the more general case where the pairs are born at arbitrary times t_{12} and t_{34}. Then we have that,

$$\begin{aligned}
\mathbf{r}_1 &= \left(-\frac{v_0}{\sqrt{2}}[\Delta t_{\rm free} + t_c - t_{12}], -\frac{v_0}{\sqrt{2}}[\Delta t_{\rm free} - t_c + t_{12}]\right), \\
\mathbf{r}_2 &= \left(\frac{v_0}{\sqrt{2}}[\Delta t_{\rm free} + t_c - t_{12}], \frac{v_0}{\sqrt{2}}[\Delta t_{\rm free} - t_c + t_{12}]\right), \\
\mathbf{r}_3 &= \left(-\frac{v_0}{\sqrt{2}}[\Delta t_{\rm free} + t_c - t_{34}], \frac{v_0}{\sqrt{2}}[\Delta t_{\rm free} - t_c + t_{34}]\right), \\
\mathbf{r}_4 &= \left(\frac{v_0}{\sqrt{2}}[\Delta t_{\rm free} + t_c - t_{34}], -\frac{v_0}{\sqrt{2}}[\Delta t_{\rm free} - t_c + t_{34}]\right).
\end{aligned} \tag{16}$$

The distance between particles becomes more complicated,

$$\begin{aligned}
d_{13}^2 = d_{24}^2 = v_0^2 \big[&t_{12}^2 + t_{34}^2 \\
&+2(t_{12} + t_{34} + \Delta t_{\rm free} - t_c)(\Delta t_{\rm free} - t_c)\big]^2 .
\end{aligned} \tag{17}$$

To proceed further we should evaluate this expression according to the distribution of possible values for t_{12} and t_{34}. This entails computing the average squared distance,

$$\overline{d_{12}^2} \propto \int_0^\infty d\tau \int_0^\infty d\tau' \; d_{12}^2 e^{-(\tau/t_{\rm sep})^2} e^{-(\tau'/t_{\rm sep})^2}. \tag{18}$$

which is defined by integrating over the decaying temporal envelope of the source term. We find,

$$\overline{d_{13}^2} = \overline{d_{24}^2} = v_0^2 \left[2(\Delta t_{\rm free} - t_c)^2 + \frac{4t'_{\rm sep}}{\sqrt{\pi}}(\Delta t_{\rm free} - t_c) + t'^2_{\rm sep}\right]. \tag{19}$$

It is then straightforward to minimize $\overline{d_{12}^2}$ with respect to $\Delta t_{\rm free}$ to obtain,

$$\Delta t_{\rm free,opt} = t_c - \frac{t'_{\rm sep}}{\sqrt{\pi}}. \tag{20}$$

and $\overline{d_{13}^2} \sim \sigma_z^2$, i.e., the particles are approximately within the typical spatial coherence length. This result has a nice interpretation: The average time for a pair to be born is $t_{\rm birth} \propto \int_0^\infty d\tau \; \tau e^{-(\tau/t'_{\rm sep})^2} = \frac{t'_{\rm sep}}{\sqrt{\pi}}$ and so the latter period of free propagation should be shortened relative to t_c by this delay time. Crucially, it corresponds precisely to the offset we have previously observed in the context of 'dephasing' of the cross-correlations at the output of the Rarity-Tapster scheme!

B. Classical particle model: ANU configuration

We can construct an analogous toy model for the current ANU experiment. First, we note that the effective interaction strength decomposes into two contributions $g(\mathbf{r}, t) = g_+(\mathbf{r}, t) + g_-(\mathbf{r}, t)$ with $g_\pm = 2U_0\psi_0(\mathbf{r}, t)\psi_\pm(\mathbf{r}, t)$ where

$$\begin{aligned}
\psi_\pm(\mathbf{r}, t) &= \sqrt{\frac{\rho_0}{3}} e^{\pm ik_0 z - i\frac{\hbar k_0^2}{2m}t} e^{-\frac{x^2}{2\sigma_{g,x}^2} - \frac{y^2}{2\sigma_{g,y}^2} - \frac{(z \mp v_0 t)^2}{2\sigma_{g,z}^2}}, \\
\psi_0(\mathbf{r}, t) &= \sqrt{\frac{\rho_0}{3}} e^{-\frac{x^2}{2\sigma_{g,x}^2} - \frac{y^2}{2\sigma_{g,y}^2} - \frac{z^2}{2\sigma_{g,z}^2}}.
\end{aligned} \tag{21}$$

In contrast to the prior UQ configuration, this source term is not peaked at the origin. Instead it is peaked at two points $\mathbf{r}_\pm(t) = (0, 0, \pm v_0 t/2)$ with $v_0 = \hbar k_0/m$, corresponding to the COM of the two separate BEC collision processes. The temporal decay remains an envelope of the form $g(\mathbf{r}, t) \sim e^{-(t/t_{\rm sep})^2}$, but now $t_{\rm sep} = 2m\sigma_{g,z}/(\hbar k_0)$ as a result of the relatively slower separation of each pair of BECs.

As a result of these features, our toy model must be altered to now describe the birth of classical particles at $\mathbf{r}_\pm(t_{\rm birth})$ with $0 \leq t_{\rm birth} \lesssim t_{\rm sep}$. Each pair of particles has momenta $\pm\mathbf{k}$ within the relevant COM frame, and for simplicity we consider the targeted pairs of the Rarity-Tapster scheme $(\mathbf{k}_1, \mathbf{k}_2)$ and $(\mathbf{k}_3, \mathbf{k}_4)$ where

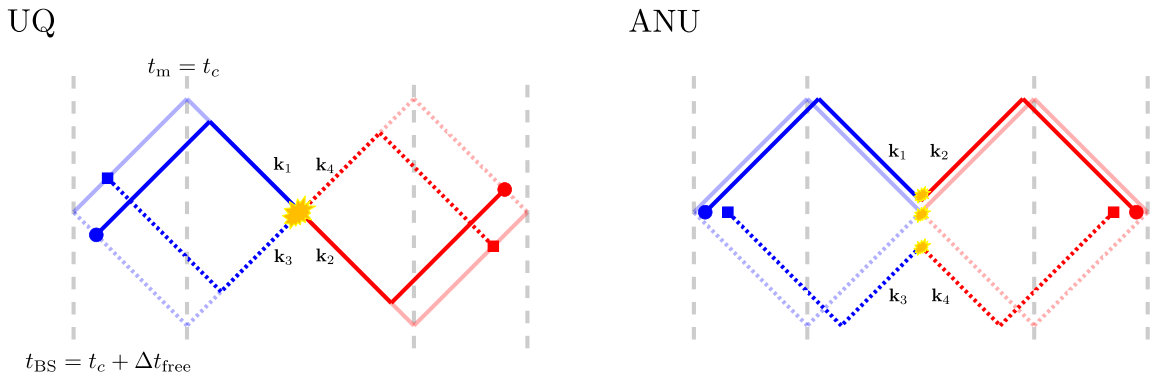

FIG. 2. A schematic of the Rarity-Tapster scheme using the classical particle model. Pairs are born at t_{12} and t_{34} respectively, before propagating through the interferometer. In the UQ configuration we assume pairs always appear at $\mathbf{r} = 0$, whereas for the ANU configuration they appear at $\mathbf{r} = \pm v_0/2 t_{12,34}$, corresponding to the origin moving in the COM frame of their respective colliding BECs. Faded lines indicate $t_{12} = t_{34} = 0$ and strong lines indicate pairs born at later $t_{12}, t_{34} > 0$. A mirror Bragg pulse is applied at t_m, which coincides with the nominal end of the BEC collision, t_c. The pairs then propagate for Δt_{free} until a beam-splitter Bragg pulse is applied at $t_{BS} = t_c + \Delta t_{free}$. For the solid lines we choose $t_{12} = 0.1 t_c$, $t_{34} = 0.3 t_c$ and indicate their positions at t_{BS} with the filled markers.

$\mathbf{k}_1 = (-k_0, k0)/2$, $\mathbf{k}_2 = (k_0, k_0)/2$, $\mathbf{k}_3 = (-k_0, -k_0)/2$ and $\mathbf{k}_4 = (k_0, -k_0)/2$.

Similar to our prior calculation, we compute the classical trajectories of the particles and obtain the spatial positions $\mathbf{r}_j$ where $j = 1, ..., 4$ identifies the initial particles with momenta $\mathbf{k}_1, ..., \mathbf{k}_4$:

$$\begin{aligned}
\mathbf{r}_1 &= \left(-\frac{v_0}{2}[\Delta t_{free} + t_c - t_{12}], \frac{v_0}{2}[\Delta t_{free} - t_c]\right), \\
\mathbf{r}_2 &= \left(\frac{v_0}{2}[\Delta t_{free} + t_c - t_{12}], \frac{v_0}{2}[\Delta t_{free} - t_c]\right), \\
\mathbf{r}_3 &= \left(-\frac{v_0}{2}[\Delta t_{free} + t_c - t_{34}], -\frac{v_0}{2}[\Delta t_{free} - t_c]\right), \\
\mathbf{r}_4 &= \left(\frac{v_0}{2}[\Delta t_{free} + t_c - t_{34}], -\frac{v_0}{2}[\Delta t_{free} - t_c]\right).
\end{aligned} \tag{22}$$

Again, we compute the distances $d_{13} = |\mathbf{r}_1 - \mathbf{r}_3|$ and $d_{24} = |\mathbf{r}_2 - \mathbf{r}_4|$, before obtaining averages $\overline{d_{13}^2}$ and $\overline{d_{24}^2}$ by integrating over the distribution of t_{12} and t_{34}, identical to our previous analysis. We find the result:

$$\overline{d_{13}^2} = \overline{d_{24}^2} = v_0^2(\Delta t_{free} - t_c)^2 + \frac{v_0^2 t_{sep}^2}{2}\left(\frac{1}{2} - \frac{1}{\pi}\right). \tag{23}$$

In contrast to the prior analysis, this expression is trivially minimized for $\Delta t_{free} = t_c$, e.g., the separation time of the BEC now plays no role. In hindsight this result is obvious: Pairs born at $t > 0$ are created at the same relative (COM) y-coordinate as pairs born at $t = 0$ and thus are not spatially delayed. Particles born at different times are only separated along the x-direction, and this motion is entirely independent of the Bragg pulses. Similar to our prior analysis of the UQ configuration, we also note that this classical model provides an elegant understanding of why "dephasing" is minimized for $\Delta t_{free} = t_c$!

C. Elucidating the contribution of spatial overlap in C_{ij}

While the previous toy models provide an elegant physical explanation of why the dephasing of the phase-sensitive correlation functions arises, how we can observe the role of indistinguishability and spatial overlap in the expressions for β_d and thus C_{ij} is still a little unclear. This is actually partially because of the fact these expressions are capturing a variety of different physical effects, including decaying correlation widths, the role of uncorrelated particles within the detection volume etc, etc. To highlight the role of spatial overlap we can rederive an approximation of our result under some aggressive and targeted assumptions.

Primarily, let us assume that $\varphi(\mathbf{k}, \mathbf{k}') \ll 1$. This is true when the free propagation duration is tuned to be very close to the optimal value, but is not a good assumption in general. Nevertheless, it is useful for our purposes here. Under this approximation we may expand the term $\cos(\Phi + \varphi(\mathbf{k}, \mathbf{k}'))$ in Eq. (6) to second order in the small parameter and then compute the integral for C_{ij}. Doing so we find that C_{ij} can be written as,

$$C_{ij} = \bar{n}^2 V + \frac{\bar{n}^2 h}{2}\left[1 \pm \cos(\Phi)\right] \alpha_x \alpha_y \beta_z' \prod_d \left(2\sigma_d^2\right), \tag{24}$$

with

$$\alpha_d = e^{-2\lambda_d^2} - 1 + \sqrt{2\pi}\lambda_d \mathrm{erf}(\sqrt{2}\lambda_d), \tag{25}$$

as previous, but now

$$\begin{aligned}
\beta_d' &= (1 - 8A^2 k_L^2 \sigma_d^2)\alpha_d \approx e^{-8A^2 k_L^2 \sigma_d^2}\alpha_d, \\
A &= \frac{\hbar}{2m}(\Delta t_{free} - t_c).
\end{aligned} \tag{26}$$

Let us ponder the argument of the exponential in the definition of β'_d. Plugging in $k_L = k_0/2$ we have $8A^2k_L^2\sigma_d^2 \equiv 2\sigma_d^2(\hbar k_0/2m)^2$. Further, realizing that for a Gaussian BEC, as defined in Appendix A and used for our calculation, $\sigma_d \equiv \sqrt{2}/\sigma_{g,z}$, we can write $8A^2k_L^2\sigma_d^2 = 4(\Delta t_{\rm free} - t_c)^2/t_{\rm sep}^2$. Substituting this form into the full expression for the correlation function we then arrive at,

$$C_{ij} = \bar{n}^2 V + \frac{\bar{n}^2 h}{2}\left[1 \pm e^{-4\left(\frac{\Delta t_{\rm free}-t_c}{t_{\rm sep}}\right)^2}\cos(\Phi)\right]\prod_d\left(2\alpha_d\sigma_d^2\right). \tag{27}$$

This final result can be elegantly understood: To observe interference in the coincidence counts at the output of the Rarity-Tapster interferometer one must ensure the free propagation time is picked such that the scattered pairs spatially overlap at the final beam-splitter.

For reference, this final expression meshes very nicely with the predictions for a Bell inequality test presented in Ref. [2]. This PhD thesis studies the Palaiseau experiment, which uses pair production in a 1D lattice. Moreover, our analysis that connects dephasing to spatial overlap is precisely what underpins the atomic HOM experiment also conducted in the Palaiseau lab [3].

IV. NUMERICAL EXAMPLES

The results of the previous sections enable us to write a succinct expression for the correlation coefficient,

$$E(\Phi) = \left.\frac{C_{14}+C_{23}-C_{12}-C_{34}}{C_{14}+C_{23}+C_{12}+C_{34}}\right|_\Phi, \tag{28}$$

$$= \frac{h\alpha_x\alpha_y\beta_z}{16\prod_d\lambda_d^2 + h\alpha_x\alpha_y\beta_z}\cos(\Phi), \tag{29}$$

with α_d and β_d as given above. This form is unchanged from Ref. [1] as all differences are encoded in β_d.

In Fig. 3 we plot the predicted behaviour of $|E(0)|$ as a function of the side length of the integration volume, which is assumed to be identical in all directions, $\Delta k_d = \Delta k$ (following the convention of the current experiment). We compare: i) the result obtained using Eqs. (9) and (10), and ii) original expressions of Ref. [1] (see Appendix B), iii) the case with no dephasing contribution [i.e., setting $\varphi(\mathbf{k},\mathbf{k}') = 0$ in Eq. (6)]. The parameters used for Fig. 3 can be found in Table I.

In the case of either trap, we observe that the amplitude of the correlation coefficient, $|E(0)|$, for the ANU scheme is generically degraded because we have not optimally chosen $\Delta t_{\rm free} = t_c$ (e.g., for the weak trap we pick $\Delta t_{\rm free} = t_c - t_{\rm sep}/\sqrt{\pi}$ motivated by the optimal choice for the UQ configuration). Nevertheless, for the small detection volumes used in the experiment we still expect strong correlations (at least relative to the ideal level).

A few broad comments should be made at this point, to put these results into the correct context. Firstly, this calculation should only be taken as a qualitative prediction. This is primarily due to the fact that the underpinning perturbative model that is used to calculate $\varphi(\mathbf{k},\mathbf{k}')$ (see Appendix A) assumes a Gaussian density profile for the source BECs. This is quantitatively incorrect for the BECs in the real experiment. Related to this, the parameter $\sigma_{g,z}$ (the rms width of the source BEC and that controls A) is not rigorously defined in terms of experimental parameters. Currently we are plugging in an estimated value for $\sigma_{g,z}$ based on the calculated Thomas-Fermi radius for the source BECs, but the scaling factor between these two has not been carefully optimized [1, 4]. Other relevant details we have ignored include the finite efficiency of the Bragg pulses and their non-zero duration.

TABLE I. Parameters for current ANU experiment.

Parameters	**Weak trap**	**Tight trap**
$(\omega_x,\omega_y,\omega_z)/(2\pi)$	$(20, 20, 20)$ Hz	$(50, 400, 400)$ Hz
N	2×10^5	2×10^5
k_0	4.1×10^6 m^{-1}	4.1×10^6 m^{-1}
(R_x, R_y, R_z)	$(48, 48, 48)$ μm	$(76, 10, 10)$ μm
$\sigma_{g,z}$	$0.58R_z$	$0.58R_z$
t_c	1 ms	130 μs
$\Delta t_{\rm free}$	0.76 ms	96 μs
$t_{\rm sep}$	0.86 ms	170 μs
h	9	2
$(\sigma_x,\sigma_y,\sigma_z)$	$(0.14, 0.13, 0.16)$ μm^{-1}	$(0.38, 5.0, 5.0)$ μm^{-1}
Δk	0.063 μm^{-1}	0.63 μm^{-1}

Figure 4 shows a calculation for $|E(0)|$ where we choose the integration volume to be scaled with the BB correlation length (i.e., we fix $\lambda_d = \lambda$ rather than $\Delta k_d = \Delta k$) and the free propagation duration $\Delta t_{\rm free}$ is allowed to vary. The purpose of this figure is to illustrate that the importance of optimally tuning $\Delta t_{\rm free}$ depends closely on the volume of the detection bin.

[1] R. J. Lewis-Swan and K. V. Kheruntsyan, Phys. Rev. A **91**, 052114 (2015).

[2] A. Imanaliev, *Towards testing Bell's inequality using atoms correlated in momentum*, Ph.D. thesis (2016), thèse de doctorat dirigée par Boiron, Denis Physique Université Paris-Saclay (ComUE) 2016.

[3] R. Lopes, A. Imanaliev, A. Aspect, M. Cheneau, D. Boiron, and C. I. Westbrook, Nature **520**, 66 (2015).

[4] J. Chwedeńczuk, P. Ziń, M. Trippenbach, A. Perrin, V. Leung, D. Boiron, and C. I. Westbrook, Phys. Rev. A **78**, 053605 (2008).

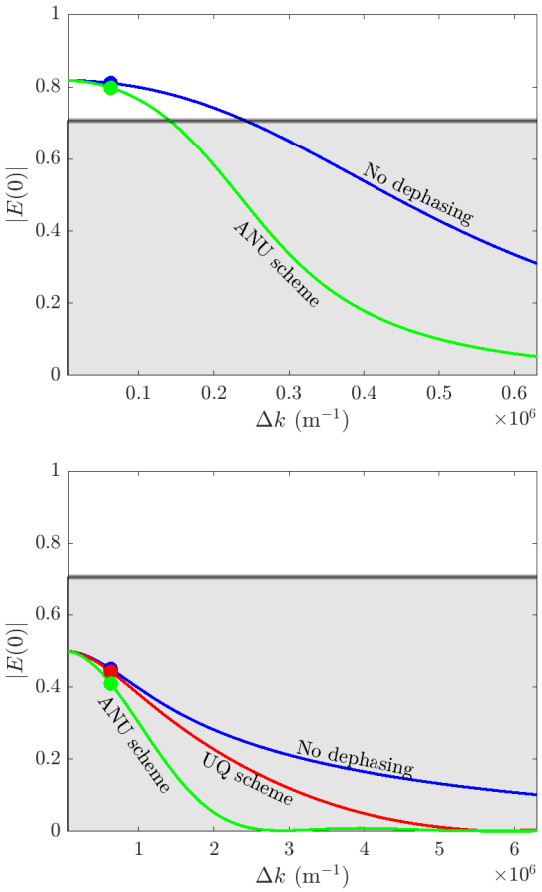

FIG. 3. Numerical prediction for amplitude of correlation coefficient in (top) weak and (bottom) tight trap configurations. Parameters for each case are given in Table I. We vary the side length of the integration volume, which is assumed to be identical in all directions, $\Delta k_d = \Delta k$. Different colored lines indicate calculated $|E(0)|$ [Eq. (29)] with: i) no dephasing contribution, and dephasing according to ii) UQ and iii) ANU schemes (see text and Appendix B). Grey shading region indicates $|E(0)| \leq 1/\sqrt{2}$, which is insufficient to achieve a violation of the CHSH-Bell inequality.

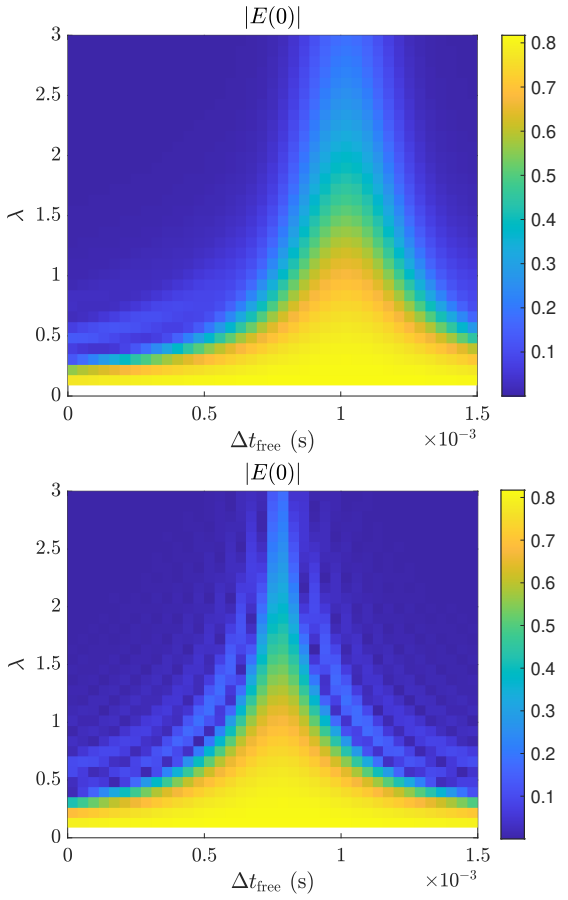

FIG. 4. Numerical prediction for amplitude of correlation coefficient in the weak trap configurations for UQ (top) and ANU (bottom) configurations. Parameters for each case are given in Table I. We vary the side length of the integration volume in an unbiased way, $\lambda_d = \lambda$. All calculations are from Eq. (29).

Appendix A: Computing the anomalous moment

We will solve for the anomalous moment $m(\mathbf{k}, \mathbf{k}', t)$ using a perturbative treatment adapted from [4]. We start from the Heisenberg equation of motion for the Bogoliubov operator $\hat{\delta}(\mathbf{r}, t)$ that describes the bosonic field in the scattering halo is,

$$i\hbar \frac{d\hat{\delta}(\mathbf{r},t)}{dt} = -\frac{\hbar^2}{2m} + g(\mathbf{r},t)\hat{\delta}^\dagger(\mathbf{r},t), \tag{A1}$$

where $g(\mathbf{r}, t)$ is a spatially and time-varying function that characterizes the colliding BECs that act as a source for the scattered atoms. For the configuration of the ANU experiment we may write $g(\mathbf{r}, t) = g_+(\mathbf{r}, t) + g_-(\mathbf{r}, t)$ where

$$g_\pm(\mathbf{r},t) = 2U_0\psi_0(\mathbf{r},t)\psi_\pm(\mathbf{r},t) \tag{A2}$$

and

$$\psi_0(\mathbf{r},t) = \sqrt{\frac{\rho_0}{3}} e^{-\frac{x^2}{2\sigma_{g,x}^2} - \frac{y^2}{2\sigma_{g,y}^2} - \frac{z^2}{2\sigma_{g,z}^2}},$$
$$\psi_\pm(\mathbf{r},t) = \sqrt{\frac{\rho_0}{3}} e^{\pm ik_0 z - i\frac{\hbar k_0^2}{2m}t} e^{-\frac{x^2}{2\sigma_{g,x}^2} - \frac{y^2}{2\sigma_{g,y}^2} - \frac{(z\mp v_0 t)^2}{2\sigma_{g,z}^2}} \tag{A3}$$

describe the BECs with COM momenta $\mathbf{k} = 0, \pm k_0 \hat{z}$, respectively, and $v_0 = \hbar k_0/m$. In this treatment, we have assumed the BECs have a Gaussian profile and this is an important simplification so that we can tractably treat the time-dependent overlap and thus separation of the source BECs (e.g., $g(\mathbf{r}, t) \to 0$ as $t \gg \sigma_{g,z}/v_0$). Moreover, our definition of $g(\mathbf{r}, t)$ explicitly ignores collisions between the BECs with $\mathbf{k} = \pm k_0 \hat{z}$, as these will not be relevant if we restrict our analysis to atoms scattered into the two primary halos. Note that our definition of $\psi_\pm(\mathbf{r}, t)$ has a different sign convention for the complex phase compared to Ref. [4]. This appears to have been notation issue that has not previously been an issue [con-

sider how part of the phase vanishes for a source term $\propto \psi_-(\mathbf{r},t)\psi_+(\mathbf{r},t)$]. It turns out that using the incorrect phase actually gives a semi-sensible answer, albeit with the source condensates moving in the wrong spatial direction, so care should !

It is straightforward to rewrite Eq. (A1) in Fourier space in terms of the bosonic operators $\hat{a}(\mathbf{k},t) = \int d^3\mathbf{r}/(2\pi)^{3/2} e^{i\mathbf{k}\cdot\mathbf{r}}\hat{\delta}(\mathbf{r},t)$, and then move to a rotating frame $\hat{b}(\mathbf{k},t) = \hat{a}(\mathbf{k},t)e^{i\hbar k^2 t/(2m)}$ to arrive at the equivalent equation of motion,

$$\frac{d\hat{b}(\mathbf{k},t)}{dt} = -\frac{i}{\hbar}\int \frac{d^3\mathbf{q}}{(2\pi)^{3/2}}\,\tilde{g}(\mathbf{q}+\mathbf{k},t)\hat{b}^\dagger(\mathbf{q},t)e^{i\hbar(k^2+q^2)t/(2m)}, \tag{A4}$$

where $k \equiv |\mathbf{k}|$. Here, we have defined $\tilde{g}(\mathbf{k},t) = \tilde{g}_+(\mathbf{k},t) + \tilde{g}_-(\mathbf{k},t)$ is the Fourier transform of $g(\mathbf{r},t)$,

$$\begin{aligned}\tilde{g}_\pm(\mathbf{k},t) &= \int \frac{d^3\mathbf{r}}{(2\pi)^{3/2}} e^{-i\mathbf{k}\cdot\mathbf{r}} g_\pm(\mathbf{r},t),\\ &= \frac{U_0\rho\sigma_{g,x}\sigma_{g,y}\sigma_{g,z}}{3\sqrt{2}} e^{-ia_\pm t - bt^2}\\ &\quad\times e^{-\frac{k_x^2\sigma_{g,x}^2}{4}-\frac{k_y^2\sigma_{g,y}^2}{4}-\frac{\sigma_{g,z}^2}{4}(k_0\mp k_z)^2},\end{aligned} \tag{A5}$$

for

$$\begin{aligned}a_\pm &= \pm\frac{\hbar k_0(k_z+k_z')}{2m},\\ b &= \frac{\hbar^2 k_0^2}{4m^2\sigma_{g,z}^2}.\end{aligned} \tag{A6}$$

Note the sign of the former was previously incorrect, and this is crucial for our solution to be physically sensible! It is useful to note that the latter parameter is connected to the intrinsic timescale of separation for the colliding BECs, $t_{\rm sep}$. In particular, we have that the momentum kick k_0 of the BECs corresponds to a velocity $v_0 = \hbar k_0/m$. Then, within the approximation of a Gaussian density profile, the time-scale for each pair of colliding BECs (e.g., one with COM momentum $\mathbf{k} = 0$ and the other with $\mathbf{k} = \pm k_0\hat{z}$) to separate is $t_{\rm sep} = 2\sigma_{g,z}/v_0 = b^{-1/2}$.

Equation (A4) can be formally integrated to yield the solution,

$$\begin{aligned}\hat{b}(\mathbf{k},t) = -\frac{i}{\hbar}\int_0^t d\tau \int \frac{d^3\mathbf{q}}{(2\pi)^{3/2}}\,\Big[&\tilde{g}(\mathbf{q}+\mathbf{k},\tau)\\ &\times \hat{b}^\dagger(\mathbf{q},\tau)e^{i\hbar(k^2+q^2)\tau/(2m)}\Big].\end{aligned} \tag{A7}$$

This form is not useful by itself, but we can invoke a perturbative approach, $\hat{b}(\mathbf{k},t) = \sum_j \hat{b}^{(j)}(\mathbf{k},t)$, and calculate relevant expectation values [4]. Using that the zeroth-order term is $\hat{b}^{(0)}(\mathbf{k},t) = \hat{b}(\mathbf{k},0)$, we can compute the anomalous moment to lowest non-trivial order,

$$\begin{aligned}M(\mathbf{k},\mathbf{k}',t) &= \langle\hat{b}(\mathbf{k},t)\hat{b}(\mathbf{k}',t)\rangle,\\ &\simeq -\frac{i}{\hbar(2\pi)^{3/2}}\int_0^t d\tau\;\tilde{g}(\mathbf{k}+\mathbf{k}',\tau)e^{i\frac{\hbar(k^2+k'^2)\tau}{2m}}.\end{aligned}$$

Plugging in Eq. (A5) and evaluating the integrals we find $M(\mathbf{k},\mathbf{k}',t) = M_+(\mathbf{k},\mathbf{k}',t) + M_-(\mathbf{k},\mathbf{k}',t)$

$$\begin{aligned}M_\pm(\mathbf{k},\mathbf{k}',t) = -i\frac{A_\pm(\mathbf{k}+\mathbf{k}')}{\sqrt{b}}\Bigg[&D_{\rm F}\left(\frac{a_\pm - c}{2\sqrt{b}}\right)\\ &+e^{-i(a_\pm - c)t - bt^2}D_{\rm F}\left(\frac{c-a_\pm+2bt}{2\sqrt{b}}\right)\Bigg],\end{aligned} \tag{A8}$$

where $D_{\rm F}$ is the Dawson F function and we have defined

$$\begin{aligned}A_\pm(\mathbf{k}) &= \frac{U_0\rho\sigma_{g,x}\sigma_{g,y}\sigma_{g,z}}{3\sqrt{2}}e^{-\frac{k_x^2\sigma_{g,x}^2}{4}-\frac{k_y^2\sigma_{g,y}^2}{4}-\frac{\sigma_{g,z}^2}{4}(k_0\mp k_z)^2}\\ c &= \frac{\hbar}{2m}(k^2+k'^2).\end{aligned} \tag{A9}$$

The anomalous moment in the original frame is then obtained as $m(\mathbf{k},\mathbf{k}',t) = M(\mathbf{k},\mathbf{k}',t)e^{-i\frac{\hbar}{2m}(k^2+k'^2)t}$.

That $M(\mathbf{k},\mathbf{k}')$ breaks into two components, $M_\pm(\mathbf{k},\mathbf{k}')$, is a reflection of the generation of back-to-back correlated pairs in two *independent* halos in the ANU experiment. In particular, inspecting Eq. (A9), we have that $M(\mathbf{k},\mathbf{k}') \simeq M_+(\mathbf{k},\mathbf{k}')$ for $\mathbf{k}+\mathbf{k}' \simeq k_0\hat{z}$ and $M(\mathbf{k},\mathbf{k}') \simeq M_-(\mathbf{k},\mathbf{k}')$ for $\mathbf{k}+\mathbf{k}' \simeq -k_0\hat{z}$.

To connect to the form proposed in Eq. (4), we would like to re-express the complex anomalous moment in terms of an amplitude and phase, e.g., $M_\pm \equiv |M_\pm|e^{i\vartheta_\pm}$. The phase is determined as

$$\begin{aligned}\vartheta_\pm(\mathbf{k},\mathbf{k}',t) = -\frac{\pi}{2} + \arg\Bigg[&D_{\rm F}\left(\frac{a_\pm - c}{2\sqrt{b}}\right)\\ &+e^{-i(a_\pm - c)t - bt^2}D_{\rm F}\left(\frac{c-a_\pm+2bt}{2\sqrt{b}}\right)\Bigg].\end{aligned} \tag{A10}$$

This expression is too complicated to be useful [i.e., the subsequent integral in Eq. (1) will become intractable]. Nevertheless, we can obtain useful insight by making a series of approximations.

First, let us assume that $(a_\pm - c)/(2\sqrt{b}) \ll \sqrt{b}t, 1$ and thus we can treat it as a small parameter and Taylor expand (A8) to lowest order. This assumption essentially requires that $|\mathbf{k}+\mathbf{k}'| - k_0 \ll 1/\sigma_{g,z}$, or equivalently that we restrict the dimensions of the integration volume in Eq. (1) for C_{ij} to be much smaller than the BB correlation width [we identify that $\sigma_z \sim 1/\sigma_{g,z}$ from Eq. (A9)]. Clearly we will not always satisfy this assumption, but nevertheless the results we generate remain useful. Second, we assume that $\sqrt{b}t \gg 1$. As was previously pointed out, this corresponds to $t/t_{\rm sep} \gg 1$ and corresponds to spatial separation of the colliding BECs. This assumption is reasonable but sometimes dubious: We typically use $t_c \simeq t_{\rm sep}$! However, the assumption allows us to gain useful insight.

Together, these assumptions give:

$$\vartheta_\pm(\mathbf{k},\mathbf{k}') \simeq -\frac{\pi}{2} - \frac{a_\pm - c}{\sqrt{\pi b}}, \tag{A11}$$

or for the anomalous moment in the original frame, $m(\mathbf{k},\mathbf{k}',t) = M(\mathbf{k},\mathbf{k}',t)e^{-i\frac{\hbar}{2m}(k^2+k'^2)t}$,

$$\theta_\pm(\mathbf{k},\mathbf{k}',t) \simeq -\frac{\pi}{2} - \frac{\hbar}{2m}(k^2+k'^2)t + \frac{\sigma_{g,z}}{\sqrt{\pi}k_0}\left[\pm k_0(k_z+k'_z) - (k^2+k'^2)\right] \quad \text{(A12)}$$

Appendix B: Previous expressions for integrated correlation function

For completeness, the integrated correlation function for the scheme proposed in Ref. [1] (UQ scheme in Fig. 1) is given by:

$$C_{ij} = \bar{n}^2 V + \frac{\bar{n}^2 h}{2}\left[1 \pm \cos(\Phi)\right]\alpha_x\alpha_y\beta_z\prod_d\left(2\sigma_d^2\right), \quad \text{(B1)}$$

This form assumes the Bragg pulses act along $\hat{z}$ and

$$\begin{aligned}\beta_d = i\sqrt{\frac{\pi}{2}}&\frac{e^{-8A^2|\mathbf{k}_L|^2\sigma_d^2}}{8\sigma_d A|\mathbf{k}_L|}\\ &\times\left[e^{-4iA|\mathbf{k}_L|\Delta k}\mathrm{erf}\left(\frac{\Delta k - 4iA|\mathbf{k}_L|\sigma_d^2}{\sqrt{2}\sigma_d}\right)\right.\\ &- e^{4iA|\mathbf{k}_L|\Delta k}\mathrm{erf}\left(\frac{\Delta k + 4iA|\mathbf{k}_L|\sigma_d^2}{\sqrt{2}\sigma_d}\right)\\ &\left.+ 2\cos(4A|\mathbf{k}_L|\Delta k)\mathrm{erf}(i2\sqrt{2}A|\mathbf{k}_L|\sigma_d)\right], \quad \text{(B2)}\end{aligned}$$

with

$$A = \frac{\hbar}{2m}\left(\Delta t_{\mathrm{free}} - t_2\right) + \frac{\sigma_{g,z}}{2|\mathbf{k}_0|\sqrt{\pi}}. \quad \text{(B3)}$$

The expression for α_d is identical for both the UQ and ANU schemes, e.g., given by Eq. (9).